International Journal of Cardiology 217 (2016) 195–204

Contents lists available at ScienceDirect

International Journal of Cardiology

journal homepage: www.elsevier.com/locate/ijcard

Worse cardiac remodeling in response to pressure overload in type 2 diabetes mellitus☆

N. Gonçalves [a,1], C. Gomes-Ferreira [a,1], C. Moura [a,b], R. Roncon-Albuquerque Jr [a], A.F. Leite-Moreira [a,c], I. Falcão-Pires [a,*]

[a] Department of Physiology and Cardiothoracic Surgery, Faculty of Medicine, Universidade do Porto, Porto, Portugal
[b] Department of Paediatric Cardiology, Centro Hospitalar São João E.P.E., Porto, Portugal
[c] Department of Cardiothoracic Surgery, Centro Hospitalar São João E.P.E., Porto, Portugal

ARTICLE INFO

Article history:
Received 5 March 2016
Received in revised form 19 April 2016
Accepted 30 April 2016
Available online 3 May 2016

Keywords:
Diabetes mellitus
Chronic pressure overload
Myocardial remodeling
Cardiac function

ABSTRACT

Background: Diabetic cardiomyopathy is characterized by cardiac structural and functional abnormalities. Additionally, chronic pressure overload conditions are highly prevalent amongst diabetic population and this association leads to a more severe myocardial impairment. The differences in myocardial pathophysiology between type 1 and type 2 diabetes mellitus (DM) still remain to be clarified. Thus, we aimed to investigate biventricular structural and functional changes promoted by the two types of DM and the impact of concomitant chronic pressure overload.

Methods: Wistar rats were injected with streptozotocin (Type 1 DM, T1DM) or fed with a hypercaloric diet (Type 2 DM, T2DM). Pressure overload was imposed in DM animals by aortic constriction and after 5 weeks of DM the cardiac function and structure were evaluated.

Results: Both types of DM promoted hypertrophy, increased fibrosis and advanced glycation end-products deposition, in the two ventricles. Interestingly, the induced myocardial alterations were distinct. While T1DM stimulated a pronounced hypertrophy and extracellular matrix remodeling, T2DM induced functional impairment. The negative impact of the association of DM with aortic constriction was more pronounced in T2DM, promoting impaired function and increased stiffness, particularly in the right ventricle.

Conclusions: Our study demonstrated that the two types of diabetes induce distinct cardiac alterations *per se* or when combined with chronic pressure overload. T1DM promoted a more extensive remodeling in cardiac structure while T2DM significantly impaired ventricular function. The impact of pressure overload was more notorious in T2DM as observed by worse myocardial remodeling, suggesting a higher susceptibility to the deleterious effects of chronic pressure overload, namely hypertension, among this diabetic population.

1. Background

Diabetes mellitus (DM) is a chronic metabolic disease that results from pancreas' inability to produce insulin, such as in Type 1 DM (T1DM), or from the incapacity of the organs to use insulin, as in Type 2 DM (T2DM). This impairment of insulin production and/or utilization and consequent hyperglycemia instigates multiple organ failure, including those of the cardiovascular system [1]. The incidence of diabetes mellitus has dramatically increased worldwide and in the next years the number of diabetic patients is expected to grow to epidemic proportions, particularly in developing countries, making it a major public health problem [2].

Despite the different triggering mechanisms, both T1DM and T2DM progress to diabetic cardiomyopathy, a condition characterized by myocardial structural and functional abnormalities in the absence of other comorbidities [3]. The role of cellular hypertrophy and extracellular matrix alterations for the development and progression of the myocardial remodeling has been described [4,5]. In fact, studies in humans [6–9] as well as in animal models [10,11] reported increased fibrosis and deposition of molecules involved in oxidative stress in both types of DM, resulting in increased myocardial stiffness. Furthermore, while T2DM impacts mostly diastolic function, T1DM has been described to mainly impair systolic function, even though we had previously described significant changes in the extracellular matrix responsible for the impaired distensibility upon stress conditions (β-adrenergic stimulation) in older T1DM rats. These initial changes in stiffness were aggravated when pressure-overload was superimposed as observed by the absence of inotropic and lusitropic response to β-adrenergic stimulation [11]. On

☆ All authors take responsibility for all aspects of the reliability and freedom from bias of the data presented and their discussed interpretation.

* Corresponding author at: Department of Physiology and Cardiothoracic Surgery, Faculty of Medicine, Universidade do Porto, Alameda Professor Hernâni Monteiro, 4200-319 Porto, Portugal.
E-mail address: ipires@med.up.pt (I. Falcão-Pires).

[1] These authors contributed equally to this work.

http://dx.doi.org/10.1016/j.ijcard.2016.04.178
0167-5273/

the other hand, the idea that T2DM first affects the diastolic function was challenged by Ernande and colleagues [12]. This group reported that 28% of a T2DM cohort presented systolic alterations although with normal diastolic function and that longitudinal systolic strain was independently associated with diabetes.

Nonetheless, comparative studies about myocardial pathophysiology of these two conditions are lacking namely concerning: i) the ventricular mechanisms responsible for the different functional outcomes; ii) the exact onset of the first myocardial manifestations and iii) the impact of diabetes on the right ventricle (RV), which has been systematically ignored in most of the existing literature, despite its probable systemic actions [13].

Several chronic disorders are common amongst T1DM and T2DM patients, being hypertension the most prevalent, affecting 40–60% of diabetic population [2,14,15]. The concomitant presence of chronic pressure overload (CPO) and DM results in more profound myocardial hypertrophy and stiffness leading to a more severe cardiomyopathy [3,11,16,17].

Additionally, most of the previous studies in diabetic cardiomyopathy focus their attention only on the impact of DM in the left ventricle (LV), neglecting the RV [13]; since DM is a systemic condition, it is expected that the RV is also affected by the metabolic impairment.

In the present work we investigate the biventricular myocardial structural and functional changes promoted by T1DM and T2DM and the impact of CPO imposed on these conditions.

2. Methods

2.1. Experimental animal model

This study was made according to the Guide for the Care and Use of Laboratory Animals published by the NIH (NIH Publication no. 85-23, revised 2011) and with the Portuguese law of animal welfare (DL 129/92, DL 197/96; P 1131/97). The Faculty of Medicine of the Universidade do Porto is a governmental institution granted with approval to perform animal experiments by the Portuguese Government.

Male Wistar Han rats were obtained from Charles River (Spain) and housed in groups of 5 *per* cage in a room at 22 °C with a controlled environment under a 12:12-h light–dark cycle and with unlimited access to food and water.

2.1.1. Chronic pressure overload

Left ventricular CPO was induced by aortic constriction in rats with 5 weeks of age (n = 20). The animals were anesthetized with sevoflurane (8% for induction and 2.5–3% for maintenance), the aorta was exposed and a blunted 23-gauge needle (0.64 mm diameter) was placed parallel to the aorta. A ligature (5-0 silk; PROLENE) was firmly tied around both the aorta and the needle. The needle was then removed, leaving the internal diameter of the aorta approximately equal to the needle.

2.1.2. Induction of diabetes mellitus

Two weeks later, 7 week-old rats were randomly divided and injected with streptozotocin (STZ; 65 mg/kg, ip; DM1 group, n = 8) or the same volume of vehicle (citrate buffer 5 mL/kg, pH = 4.5; CT1 group, n = 9). Half of the banded animals also received STZ resulting in an additional group (DB1, n = 7).

To induce T2DM, 7 week-old rats were randomly divided and fed with a hypercaloric diet rich in lipids, carbohydrates and increase salt content (5.4 kcal/g, F2685, BioServe, DM2 group, n = 10) or a regular diet (2.9 kcal/g, A04; Scientific Animal Food & Engineering; CT2 group, n = 10). Half of the banded animals were also fed with this hypercaloric diet resulting in an additional group (DB2, n = 13). The detailed diet composition is described in Table 1.

Table 1
Diet composition.

	Regular diet (AO4)	Hypercaloric diet (F2685)
Calorie composition (kcal/g)	2.9	5.4
Protein (%)	16.1	20.5
Carbohydrate (%)	3.2	34.7
Monosaccharides (gm/kg)	17.3	1
Disaccharides (gm/kg)	6.8	182
Polysaccharides (gm/kg)	26.1	157
Fat (%)	3.1	36.0
Saturated fat (gm/kg)	6.5	141
Monounsaturated fat (gm/kg)	20.0	162
Polyunsaturated fat (gm/kg)	1.2	40.2
Sodium (%)	0.25	0.4

The presence of DM was confirmed by plasma glycemia > 250 mg/dL (Breeze, Bayer). Five weeks later cardiac structure and function were evaluated and samples collected.

The experimental groups resultant from this protocol design are described in Table 2.

2.2. Echocardiogaphic assessment

Echocardiographic evaluation was performed using a 10 MHz transducer (GE Vivid 7). Animals were anesthetized (ketamine:xylazine, 75:5 mg/kg, ip) and allowed to stabilize for 15 min. From the left parasternal short-axis view, two-dimensional guided M-mode tracings were made just below the mitral valve at the level of the papillary muscles for measurements of the interventricular septum (IVS, mm), posterior wall thickness (LVPW, mm) and left ventricular diameter (LVD, mm) during systole and diastole. Left ventricular mass (LVM, mg) was calculated by the formula $= 1.04 \times (\mathrm{IVSd} + \mathrm{LVDd} + \mathrm{LVPWd})^3 - \mathrm{LVD}^3$. All these parameters were normalized to body surface area (IVSI, LVPWI, LVDI and LVMI) as described previously [11]. Three representative cycles were measured *per* rat and their average was calculated.

2.3. Hemodynamic evaluation

The animals were anesthetized with sevoflurane (8% for induction and 2.5–3% for maintenance), intubated for mechanical ventilation (Dual Mode, Kent Scientific), and placed over a heating pad (body temperature was maintained at 37 °C). To compensate for the perioperative losses, the right jugular vein was cannulated for fluid administration (prewarmed 0.9% NaCl solution, 10 mL/kg/h). A median sternotomy was made and the aorta dissected for record flux with an ultrasonic flow probe, connected to a flowmeter (Transonic Systems Ithaca). High-fidelity tip pressure–volume catheters were inserted into the LV and RV (SPR-847, 2F and PVR-1045, 1F respectively; Millar Instruments). After complete instrumentation, the animal was allowed to stabilize for 15 min. Data was continually acquired digitally (MPVS 300, Millar Instruments), recorded at 1000 Hz (ML880 PowerLab 16/30, Millar instruments), and analyzed off-line by software PVAN 3.5 (Millar Instruments).

Hemodynamic recordings were made under basal conditions with respiration suspended at end-expiration. The hemodynamic parameters analyzed were the peak systolic pressure (P_{Syst}), maximum rate of pressure rise (dP/dt_{max}), end-diastolic pressure (EDP) and time constant of isovolumetric relaxation (Tau). Ascending aorta occlusions were performed during the diastole separating two heartbeats. The first beat was control, and the second beat was test heartbeat. The contractile reserve was then calculated as the % of increase of the systolic pressure according to the formula: [(P_{Syst} of the second beat − P_{Syst} of the first beat) / P_{Syst} of the first beat)] × 100. This intervention evaluates the effect of increased afterload without changes of preload or long-term load history. Conductance Calibration: Parallel conductance values were obtained by the injection of approximately 100 μL of 10% NaCl into

Table 2
Protocol design and the resultant experimental groups (CT1, DM1, DM1, CT2, DM2 and DB2).

Procedure	CT1	DM1	DB1	CT2	DM2	DB2
Pressure overload (week 0)	–	–	Aortic banding	–	–	Aortic banding
Diabetes induction (week 2)	Normal diet + citrate buffer	Normal diet + STZ (65 mg/kg)	Normal diet + STZ (65 mg/kg)	Normal diet (2.9 kcal/g)	Hypercaloric diet (5.4 kcal/g)	Hypercaloric diet (5.4 kcal/g)
Cardiac evaluation sample collection (week 7)	✓	✓	✓	✓	✓	✓

the right atrium. Calibration from Relative Volume Unit (RVU) conductance signal to absolute volumes (μL) was undertaken using a previously validated method of comparison to known volumes in Perspex wells [18].

2.4. Sample collection and morphometric analysis

At the end of the hemodynamic evaluation, blood and tissue samples of all animals were collected. The heart and lungs were excised, weighed and stored at −80 °C for functional studies using isolated cardiomyocytes or fixed in 10% buffered formalin for histologic procedures. Morphometric data was normalized to body weight (BW).

2.5. Quantitative histomorphometry

Tissue samples were fixed, dehydrated with graded ethanol, cleared with xylene and included in paraffin blocks. Serial sections (4 μm of thickness) of paraffin blocks were cut by a microtome (RM2125RTS, Leica) and mounted on silane-coated slides. The slides were observed at light microscopy (Dialux 20, Leitz) and images recorded to posterior analysis.

Cardiomyocytes diameter from both ventricles was measured (cell B, Olympus) at the nucleus level in 50 representative myocytes for each animal in hematoxylin-and-eosin stained samples.

The percentage of myocardial fibrosis was calculated (ImagePro, MediaCybernetics) as the sum of all connective tissue areas divided by the sum of connective tissue and muscle areas averaged. Six representative fields of each picrosirius red stained samples from both ventricles were analyzed and areas of reparative and perivascular fibrosis were excluded.

Advanced glycation end-products (AGE) immunohistochemistry was performed in sliced heart sections after antigen retrieval with 10 mM sodium citrate buffer. Blockage of endogenous activity was performed using a 3% hydrogen peroxide solution in methanol, 5% normal goat serum (ab7481, abcam) and with an endogenous avidin + biotin blocking system (ab3387, abcam). The slices were incubated overnight with anti-AGE primary antibody (1/5000, ab23722, abcam) at 4 °C, for 2 h with the secondary antibody (goat anti-rabbit IgG, 1/250, ab6720, abcam) and with 3.3-diaminobenzidine (DAB, ab94665, abcam). The counterstained was performed with Gill hematoxylin (Merck) and in the negative control, the primary antibody was omitted. AGE quantification was performed in 6 representative images of each animal from both ventricles using ImagePro software (MediaCybernetics).

2.6. Isolated cardiomyocyte measurements

Force measurements were performed in single, triton-permeabilized cardiomyocytes mechanically isolated as described previously with adaptations [19]. Briefly, myocardial samples from LV and RV were defrosted in extraction solution (without Ca^{2+}), mechanically disrupted and incubated for 5 min in relaxing solution supplemented with 0.2% Triton X-100 to remove all membrane structures. The cardiomyocytes were then washed by consecutive centrifugations and attached between a force transducer and a motor. An image of the cardiomyocyte was obtained by a video camera and the width, high and sarcomere length of the cell calculated by the software (ASI, Aurora Systems). Cross-sectional area was calculated assuming an elliptical shape of the cell.

Data acquisition was obtained after transferring the cardiomyocyte from relaxing (pCa ($-\log10[Ca^{2+}]$) = 9.0) to activating solution (pCa = 4.5). In this activating solution the isometric force started to develop and once a steady-state force level was reached, the cell was shortened within 1 ms to 80% of its original length (slack test) to determine the baseline of the force transducer. The distance between the baseline and the steady force level is the total force (F_{Total}). The cell was placed again in the relaxing solution; re-acquiring its resting length and a second slack test of 10 s duration was performed to determine resting or passive force ($F_{Passive}$). Active force (F_{Active}) was calculated using the formula: $F_{Total} = F_{Active} + F_{Passive}$. All force values were then normalized to the corresponding cross-sectional area of the cardiomyocyte. In average 30 cardiomyocytes were measured per group (~5 cardiomyocytes per animal in a total of 6 animals of each group).

2.7. Statistical analysis

All data are presented as mean ± SEM and n represents the number of animals. Differences within T1DM and T2DM protocols were analyzed with 1 way ANOVA, confirming normality and homogeneity of variance with Shapiro–Wilk and F tests respectively (GraphPad Prism v.6). Significance level was set at $p < 0.05$.

3. Results

3.1. Morphometric characterization

All animals with T1DM presented lower BW but increased heart, lung and renal indexed weight (Table 3). The simultaneous presence of pressure overload had no impact in the parameters mentioned before. The ingestion of a HCD for 5 weeks did not alter body weight of the DM2 animals, neither the weight of other organs analyzed. On the contrary, the DB2 group presented cardiac hypertrophy and evidences of lung congestion.

3.2. Cardiac structure

Echocardiographic results of both protocols are summarized in Fig. 1. The cardiac hypertrophy previously reported in DM1 was further verified by increased LVMI (Fig. 1H). According to indexed heart weight, also LVMI was similar to control in DM2, although a concentric pattern of hypertrophy was already ongoing, as observed by the increased IVSI and LVPWI alongside with significant reduction in chamber diameter (Fig. 1). As expected aortic banding promoted further hypertrophy in both protocols (DB1 and DB2 groups). No differences in heart weight were detected in the T1DM protocol or the T2DM protocol.

The histological assessment demonstrated that, independently of the protocol, diabetes promoted increase of cardiomyocyte diameter in both ventricles (Fig. 2A and D). This cellular alteration was evident in a greater extent in the animals with aortic banding. Interestingly, hypertrophy was already evident at the cell level in DM2 despite unchanged LVMI. Moreover, we verified that the percentage of cell hypertrophy was superior in DM1 animals compared to CT1 group in

the left (DM1: 21% vs DM2: 7% increase) and in the right ventricle (DM1: 12% vs DM2: 6% increase).

Regarding the extracellular matrix, all experimental groups presented higher fibrosis and AGE content when compared to the respective control group (Fig. 2). This myocardial remodeling occurred with the same magnitude for both protocols in the LV, however in the RV, the increase of fibrosis was greater in both diabetic groups versus control animals (DM1: 81% vs DM2: 30% and DB1: 74% vs DB2: 25% increase).

3.3. Biventricular function

As detailed in the left panel of Fig. 3 the systolic and diastolic functions of the left ventricle in baseline conditions were preserved in DM1 as well as in DM2 animals. Banding promoted, as expected, increased peak systolic pressure in both DB groups. In addition, DB2 group presented a significant reduction in the LV contractile reserve (isovolumetric contractions; CT2: 69.6 ± 4.7%, DM2: 63.5 ± 7.7%, DB2: 36.3 ± 8.2%, $p = 0.036$ versus CT2), as well as increase stiffness (EDP) and impaired relaxation (Fig. 3C and D).

Concerning the RV (Fig. 3 right panel), no significant differences were observed in T1DM protocol. Contrarily, T2DM markedly impaired relaxation and, upon chronic pressure overload, RV function further deteriorated, as observed by a significant increase in both peak systolic and end-diastolic pressures.

Finally, the studies performed in permeabilized cardiomyocytes (Fig. 4), which allow us to detect functional changes at the myofilamentary level, revealed that 5 weeks of T1DM induced a significant increase in RV $F_{Passive}$ (Fig. 4D). Contrarily, in T2DM, despite an evident tendency, significant differences were only observed biventricularly in active and passive forces when CPO was imposed (DB2 group).

4. Discussion

Since the recognition of diabetic cardiomyopathy in the 1970s [20], researchers have tried to unravel the mechanisms instigating this disease. However, the majority of the papers focus their attention in one type of DM and in one ventricle, neglecting the importance of the RV for myocardial function. In our study we used two well-known animal models of DM and compared the magnitude of the biventricular adaptations triggered either by T1DM or T2DM. Furthermore, since the prevalence of hypertension among DM patients is elevated [2], we imposed CPO to diabetic animals to assess the cardiac impact of their concomitant presence. Finally, in order to better understand the level of the adaptations triggered in each type of DM we used an approach from the *in vivo* to the *in vitro* myofilamentary level.

In our protocol the T1DM and T2DM induced remodeling of the LV with cardiac hypertrophy as well as increased fibrosis and AGE deposition, in agreement with the literature [1,21]. Interestingly, we observed that these myocardial structural alterations were also present in the RV. Moreover, T1DM stimulated more pronounced hypertrophy, with bigger percentage increase of cardiomyocyte diameter and fibrosis content compared to T2DM. When we combined DM with CPO the most notorious impact was observed in the T2DM model. The simultaneous presence of these two risk factors (DB2 group) affected especially the RV, promoting an elevation of peak systolic pressure, impaired relaxation and increased cardiomyocyte stiffness, while in the LV reduced contractile reserve and increased myocardial stiffness were observed (EDP and $F_{Passive}$).

To our knowledge, among the scarce studies comparing the cardiac effects of both types of DM, the most relevant one was performed by Radovits et al. [22,23], who used STZ as a T1DM model and ZDF rats to evaluate the influence of T2DM. Compared to our protocol design some differences might have contributed to the distinct outcomes reported by this author, namely the T2DM model (genetic vs nutritional model), the heterogeneity of animal age at the beginning of protocol (20 and 30 vs 7 weeks) and the duration of the DM (8 and 30 vs 5 weeks of DM). In our study we used only one strain of rats (Wistar Han) in order to specifically address the myocardial effect of each type of DM, without other confounding factors related to the animal strain.

4.1. Cardiac alterations promoted by T1DM

Our DM1 animals presented cardiac hypertrophy further confirmed in histological analysis by enlarged LV cardiomyocytes. The LV pro-hypertrophic outcome in T1DM has been widely demonstrated in several animal models [11,24] as well as in clinical studies [25]. Similarly in Radovits study [23] the animals injected with STZ exhibited an increase in cardiomyocyte width (8.3%). The authors proposed that the molecular mechanism triggering the hypertrophic pathway might be through the shift in the production of α-MHC in favor of the fetal β-MHC isoform. Additionally, our histological assessment demonstrated that, not only the myocytes from the LV were enlarged in the DM1 animals but also the ones from the RV, highlighting the systemic effects of the disease.

Another important aspect implicated in myocardial remodeling in the context of DM is the deposition of fibrosis and AGE as observed biventricularly in this protocol. These features in T1DM1 were already described by others, in fact, elevated LV fibrosis and nitrotyrosine, a marker for nitrooxidative stress, were reported in the same animal model [22]. The authors of this study demonstrated that contributing to fibrosis-increase deposition was TGF-β signaling pathway. However, further molecular studies need to be done to fully understand the mediators responsible for the remodeling in the context of T1DM.

In our 5-week protocol of T1DM, the animals exhibited preserved systolic and diastolic functions with no alterations in the parameters analyzed. These results are in line with our previous results in the LV of older animals but with the same duration of T1DM [11]. Conversely other authors reported impaired cardiac function (decreased dP/dt_{max}, dP/dt_{min}, and Tau) as soon as 2 to 3 weeks after STZ injection [26,27] and even before LV myocardial content is altered [27]. However, several differences can explain the divergent results as both studies were performed in older rats from a different strain, the STZ dose was lower and the measurements were made in conscious animals.

The RV of the DM1 group presented hypertrophic and stiffer cardiomyocyte ($F_{Passive}$). Interestingly, despite the presence of RV fibrosis and increased $F_{Passive}$, the global diastolic function was only marginally affected as observed by the tendency for RV relaxation impairment and EDP increase. Ventricular systolic function was similar to control group. Only a few studies in DM presented data related to the RV, particularly in the T1DM so that, to our knowledge, our study is the first to characterize changes in the right ventricle.

Table 3
Morphometric data.

	CT1	DM1	DB1	CT2	DM2	DB2
Body weight (g)	408 ± 14	245 ± 8 α	247 ± 14 α	310 ± 14	322 ± 11	318 ± 8
Heart/BW (g/kg)	2.6 ± 0.06	3.1 ± 0.08 α	3.5 ± 0.25 α	2.9 ± 0.10	2.9 ± 0.08	4.4 ± 0.25 §†
Lung/BW (g/kg)	3.4 ± 0.15	5.0 ± 0.21 α	4.5 ± 0.16 α	4.5 ± 0.17	3.8 ± 0.36	5.5 ± 0.33 †
Kidney/BW (g/kg)	2.7 ± 0.10	5.1 ± 0.17 α	4.8 ± 0.20 α	3.1 ± 0.09	3.2 ± 0.09	3.0 ± 0.10

BW: body weight. The values are represented as means ± SEM. $p < 0.05$: α vs CT1, β vs DM1; § vs CT2, † vs DM2.

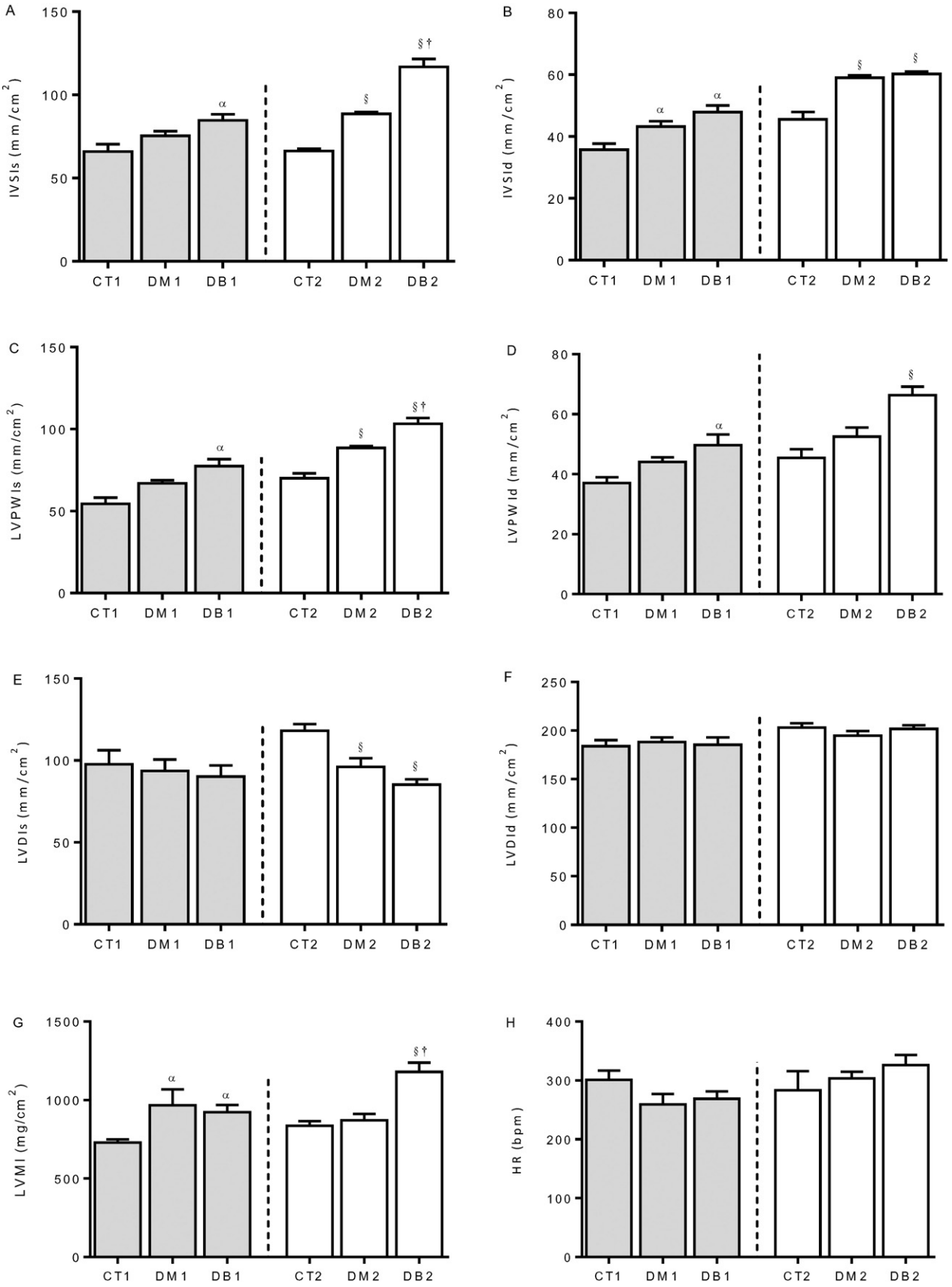

Fig. 1. Left ventricle echocardiographic assessment. HR, heart rate; IVSI, interventricular septum thickness index; LV, left ventricular; LVDI, LV diameter index; LVMI, LV mass index; LVPWI, LV posterior wall thickness index. The parameters were obtained in systole (left panel) and in diastole (right panel). The values are represented as means ± SEM. $p < 0.05$: α vs CT1, β vs DM1; § vs CT2, † vs DM2.

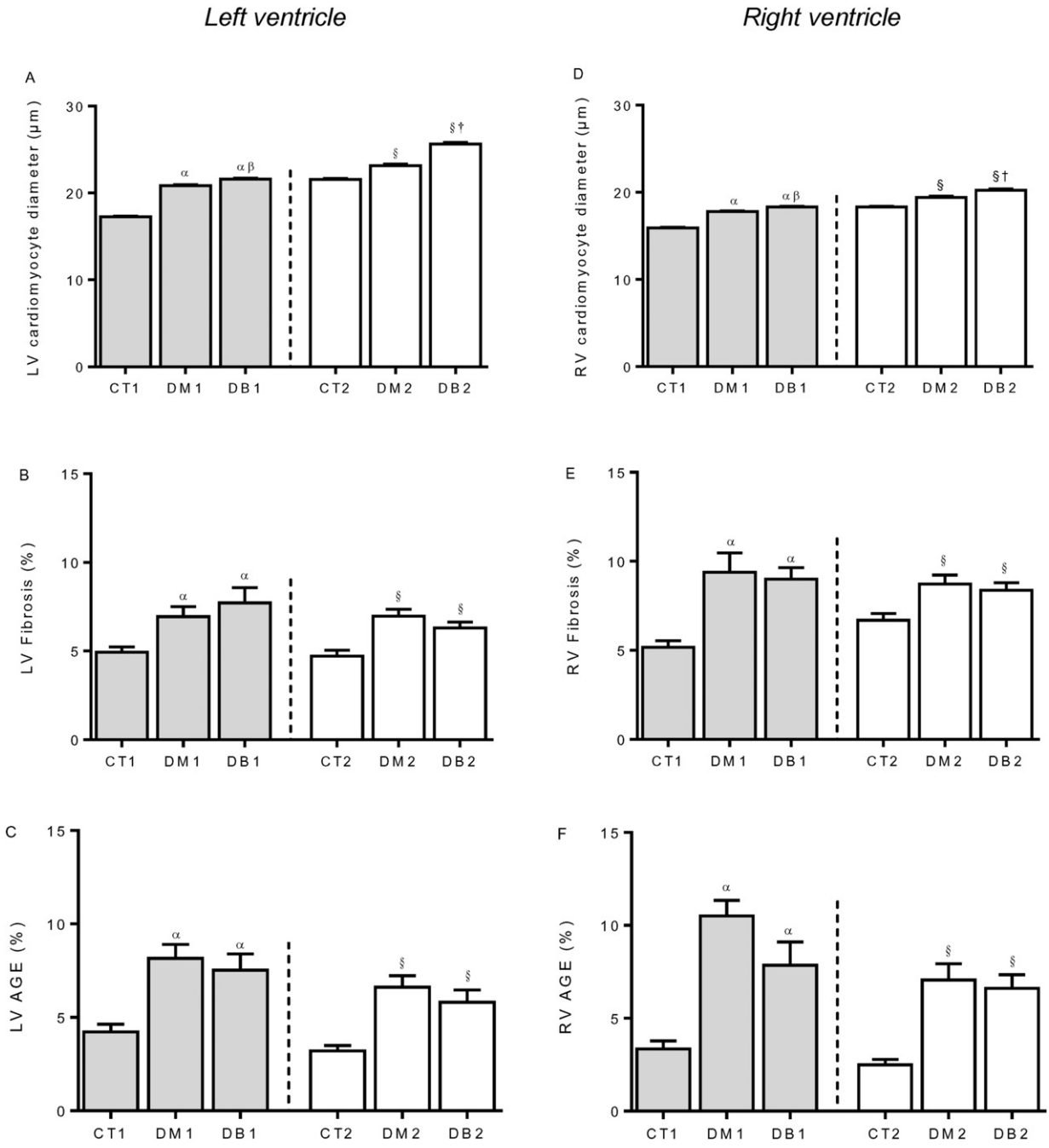

Fig. 2. Left and right ventricular histological assessment (left and right panels, respectively) of: cardiomyocytes hypertrophy (A and D); interstitial fibrosis (B and E) and advanced glycation end-products (AGE, C and F). The values are represented as means ± SEM. $p < 0.05$: α vs CT1, β vs DM1; § vs CT2, † vs DM2.

Finally, CPO imposed on T1DM promoted increased LV peak systolic pressure and a higher extent of cardiomyocyte hypertrophy, a direct consequence of the increased afterload imposed by aortic constriction. No other differences of the structural and functional parameters evaluated were detected, revealing that the simultaneous presence of T1DM and pressure overload adds no extra deleterious cardiac effects to the ones triggered by T1DM alone.

4.2. Myocardium adaptations induced by T2DM

In our study we chose to use a HCD to induce T2DM rather than a genetically modified animal model as we found it physiologically and epidemiologically more relevant. This choice was made in face of the world wide scenario of increasing population with overweight or obesity and related comorbidities. The increase in T2DM prevalence has been associated with a sedentary lifestyle and consumption of diets rich in fat and sugars. Indeed, T2DM represents more than 90% of the diabetic patients [28]. We believe that discovering the mechanisms, as well as identifying the onset of the first myocardial repercussions of these diets, is important not only to prevent, but also to modulate the progression of diabetic cardiomyopathy in an earlier stage.

After 5 weeks of nutritional modulation, the animals presented similar body weight compared to the control group, however hyperglycemia, glucose intolerance and insulin resistance were already present as we previously reported, denoting T2DM [29]. The echocardiographic evaluations performed in the LV of the DM2 group revealed cardiac concentric hypertrophy (increased wall thickness and decrease chamber diameter) although similar heart weight compared to the CT2 animals.

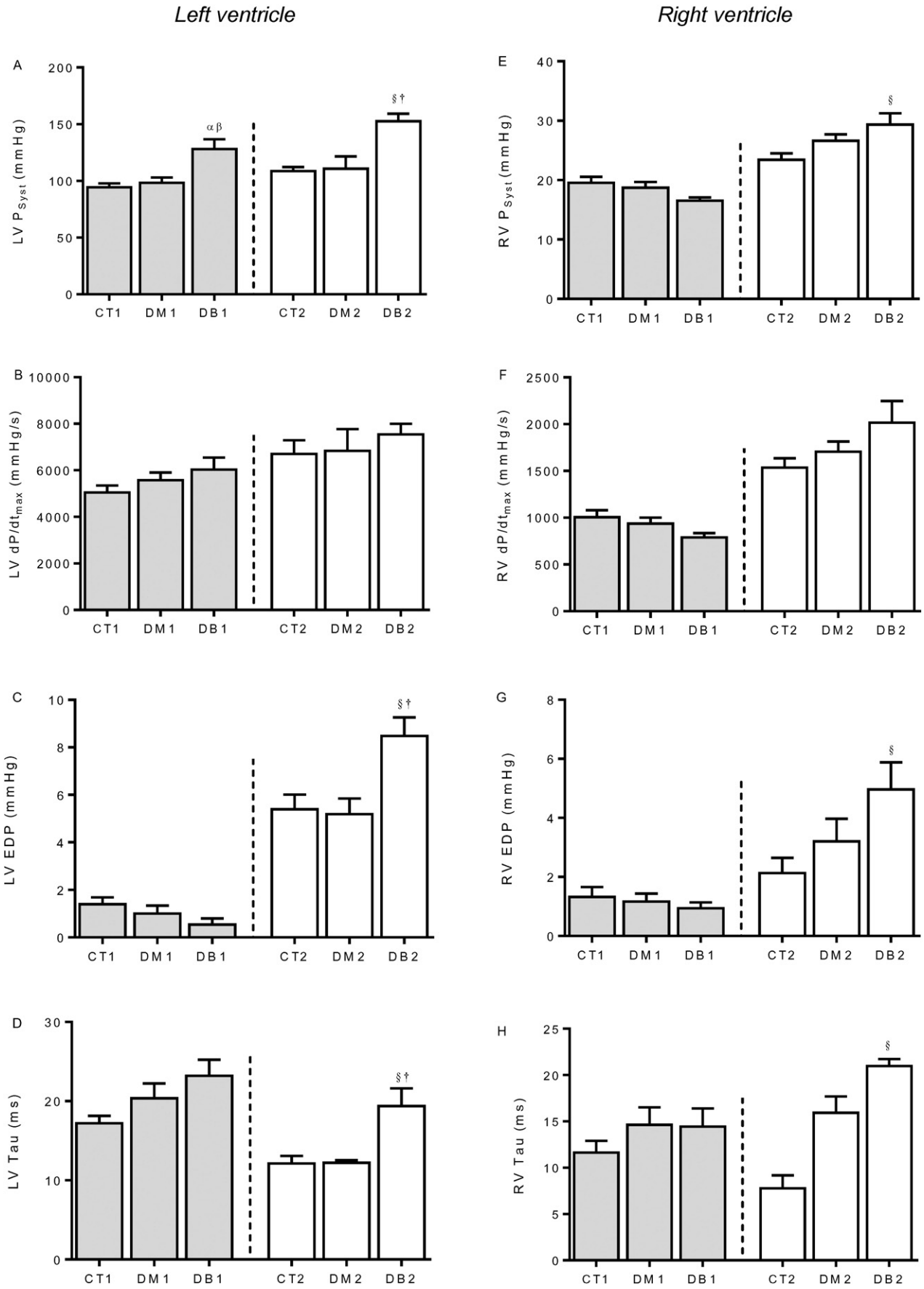

Fig. 3. Baseline hemodynamic evaluation of the left and the right ventricle (left and right panels, respectively) of: peak systolic pressure (P_{Syst}, A and E), maximum rate of pressure rise (dP/dt_{max}, B and F), end-diastolic pressure (EDP, C and G) and time constant of isovolumetric relaxation (Tau, D and H) under baseline conditions. The values are represented as means ± SEM. $p < 0.05$: α vs CT1, β vs DM1; § vs CT2, † vs DM2.

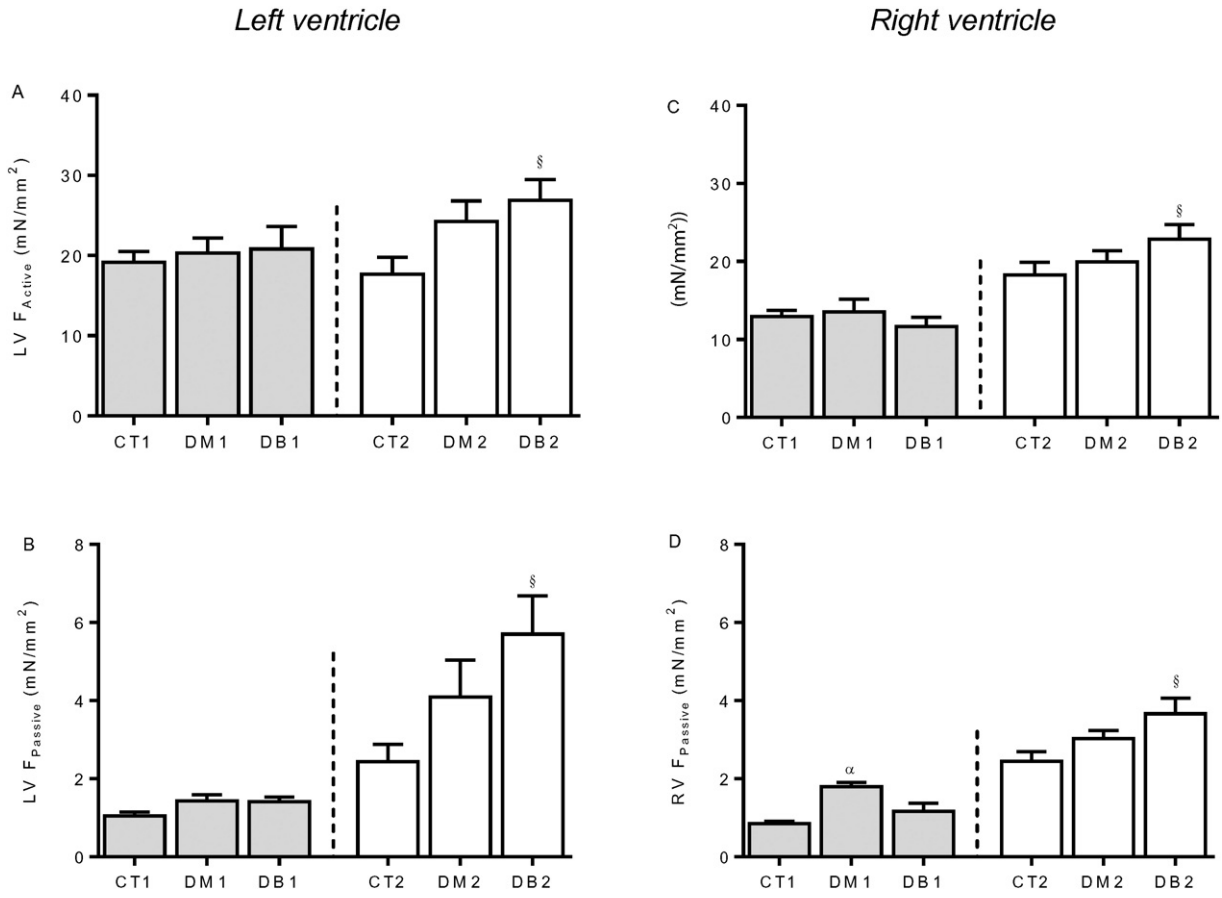

Fig. 4. Data from permeabilized cardiomyocytes from the left and the right ventricles (left and right panels, respectively), namely, active force (F_{Active}, A and C) and passive force ($F_{Passive}$, B and D). The values are represented as means ± SEM. $p < 0.05$: α vs CT1, β vs DM1; § vs CT2, † vs DM2.

Additionally, the ECM was also altered with high content of fibrosis and AGE. The activation of pro-hypertrophic and pro-fibrotic pathways is a characteristic shared in nutritional as well as in genetic models of T2DM. ZDF animals were reported to have an increase of 6.4% in LV cardiomyocyte width and of 45% in fibrosis score [23]. In addition, a high-fat diet-induced obesity mice model also showed elevated heart mass, cardiomyocyte hypertrophy and cardiac fibrosis [30]. Furthermore, independently of the type of DM [24,31], one of the diabetic cellular metabolic disorders is the increased oxidative stress with elevated production of AGE that highly contribute to the progression of diabetic cardiomyopathy, being also related with myocardial fibrosis. In fact, animal models of T2DM [13,23] as well as myocardial biopsies [7] presented increased ROS production and altered antioxidant mediators [5]. All the LV structural changes mentioned before were also observed in the RV, namely cardiomyocyte hypertrophy and ECM remodeling (high fibrosis and AGE deposition compared to CT2 group). Despite these structural changes, systolic and diastolic functions were preserved in DM2 group.

In our protocol, the tendency for dysfunction observed in the RV of the DM2 group was exacerbated and becomes significant only when combined with pressure overload. Indeed, DB2 animals presented increased RV EDP as well as impaired relaxation. Conversely, in a previous study performed in a genetic model of obesity and T2DM, 14 week-old ZDF rats showed evidences of decreased systolic function in both ventricles, with depressed LV fractional shortening and tricuspid annular plane systolic excursion [13]. In this animal model, where the hyperglycemic period lasts longer, metabolic/endocrine impairment of the adipose tissue was already evident [32]. Indeed, these authors were able to correlate systolic dysfunction of both ventricles with impaired glucose metabolism and insulin signaling [13]. The differences between these studies and our results are probably related with the animal model used and the duration of the metabolic dysfunction. In humans, this impaired biventricular contractile function was similarly observed in a report using 157 T2DM patient [33]. However, our goal in this study was to characterize early cardiac changes induced by metabolic dysfunction, before obesity or overweight is established.

When CPO and T2DM coexist, the functional changes were evident at the myofilamentary level promoting biventricular increased F_{Active} and $F_{Passive}$. Interestingly, in diastolic heart failure patients, elevated $F_{Passive}$ was equally reported and associated with extensive myocardial stiffness and elevated LV EDP [34]. These patients are characterized by concentric cardiac hypertrophy [35] with bigger cardiomyocytes, and fibrosis deposition, in the same fashion as the DB2 animals. This similar pattern of structural and functional changes demonstrates that underlying diastolic and diabetic cardiomyopathy are identical pathophysiological mechanisms. Another important factor contributing to bigger $F_{Passive}$ is oxidative stress. In fact, it has been reported that the oxidative-stress environment observed in DM promotes posttranslational modifications in sarcomeric contractile proteins [36], contributing to function impairment. Further cell-based studies involving antioxidant agents are needed to better unravel the contribution of ROS in cardiac dysfunction.

4.3. Comparison of the biventricular impact of T1DM vs T2DM

In this study we compared the actual severity in cardiac structure and function of both DM types, particularly when combined with CPO. We observed that T1DM have a higher impact in cardiac structure compared to T2DM. Conversely, the presence of pressure overload is more deleterious in T2DM. Indeed, the DB2 animals exhibited biventricular

changes in the myofilamentary function presenting increased stiffness ($F_{Passive}$) and higher contractility (F_{Active}). Interestingly, the association of the two pathologies induced global ventricular systolic and diastolic dysfunctions, particularly in the RV.

One of the limitations of our study is the extent of functional characterization, particularly of the RV. An urgent need for the development of noninvasive methods and/or techniques that allow a more accurate biventricular functional assessment is recognized in diverse small animal models. Also, a better understanding of the real cardiac impact of DM and its underlying molecular pathways urge, aiming for personalized medicine/therapies. Lastly, we used two animal models of DM without glycemic control and this is not representative of the clinic scenario since most of the patients with DM are under insulin treatment.

Nevertheless, our study contributed to understanding the actual relevance of glycemia control, mainly in T1DM patients to prevent cardiac hypertrophy. In T2DM we have shown the importance of an early detection of the metabolic disarrangements that precede diabetes and to strictly control blood pressure among T2DM patients.

5. Conclusion

In conclusion, our study demonstrates that both types of diabetes induce distinct cardiac alterations *per se* and when combined with chronic pressure overload. The T1DM promotes a more pronounced hypertrophy and extracellular matrix remodeling, whereas T2DM has higher impact in myocardial function, either in the LV as in the RV. The simultaneous presence of pressure overload had cardiac repercussions only in the DB2 group, impairing biventricular systolic and diastolic functions.

Funding

This work was supported by Portuguese Foundation for Science and Technology Grant UID/IC/00051/2013 financed with national funds by Fundação para a Ciência e Tecnologia and by Fundo Europeu de Desenvolvimento Regional through COMPETE 2020 – Programa Operacional Competitividade e Internacionalização (POCI), EXCL-II/BIM-MEC/0055/2012, and by European Commission Grant FP7-Health-2010, MEDIA-261409. This work was supported by Portuguese Foundation for Science and Technology Grant SFRH/BD/66628/2009 (to N. Gonçalves).

Competing and conflicting interests

The authors declare that they have no conflict of interests.

Author contribution

Nádia Gonçalves: conception and design of research; performed experiments; analyzed data; interpreted results of experiments; prepared figures; drafted manuscript, approved final version of manuscript.

Carla Gomes-Ferreira: performed experiments; analyzed data; prepared figures; drafted manuscript, approved final version of manuscript.

Cláudia Moura: performed experiments; analyzed data, approved final version of manuscript.

Roberto Roncon-Albuquerque Jr: conception and design of research; interpreted results of experiments, edited and revised manuscript, approved final version of manuscript.

Adelino F. Leite-Moreira: conception and design of research; edited and revised manuscript, approved final version of manuscript.

Inês Falcão-Pires: conception and design of research; performed experiments; analyzed data; interpreted results of experiments; prepared figures; edited and revised manuscript, approved final version of manuscript.

Acknowledgments

The authors thank Ana Filipa Silva and Cláudia Mendes for the cardiac histological evaluation and Patrícia Gonçalves Rodrigues for isolated cardiomyocyte's analysis. The authors thank André Lourenço for the statistical analysis.

References

[1] T. Miki, S. Yuda, H. Kouzu, T. Miura, Diabetic cardiomyopathy: pathophysiology and clinical features, Heart Fail. Rev. 18 (2013) 149–166.
[2] M. Authors/Task Force, L. Ryden, P.J. Grant, S.D. Anker, C. Berne, F. Cosentino, et al., ESC Guidelines on diabetes, pre-diabetes, and cardiovascular diseases developed in collaboration with the EASD: the Task Force on diabetes, pre-diabetes, and cardiovascular diseases of the European Society of Cardiology (ESC) and developed in collaboration with the European Association for the Study of Diabetes (EASD), Eur. Heart J. 34 (2013) 3035–3087.
[3] S. Boudina, E.D. Abel, Diabetic cardiomyopathy revisited, Circulation 115 (2007) 3213–3223.
[4] B.K. Tiwari, K.B. Pandey, A.B. Abidi, S.I. Rizvi, Markers of oxidative stress during diabetes mellitus, J. Biomark. 2013 (2013) 378790.
[5] D.M. Ansley, B. Wang, Oxidative stress and myocardial injury in the diabetic heart, J. Pathol. 229 (2013) 232–241.
[6] J. Nozynski, M. Zakliczynski, D. Konecka-Mrowka, T. Zielinska, H. Zakliczynska, B. Nikiel, et al., Advanced glycation end product accumulation in the cardiomyocytes of heart failure patients with and without diabetes, Ann. Transplant. 17 (2012) 53–61.
[7] L. van Heerebeek, N. Hamdani, M.L. Handoko, I. Falcao-Pires, R.J. Musters, K. Kupreishvili, et al., Diastolic stiffness of the failing diabetic heart: importance of fibrosis, advanced glycation end products, and myocyte resting tension, Circulation 117 (2008) 43–51.
[8] S. Willemsen, J.W. Hartog, Y.M. Hummel, M.H. van Ruijven, I.C. van der Horst, D.J. van Veldhuisen, et al., Tissue advanced glycation end products are associated with diastolic function and aerobic exercise capacity in diabetic heart failure patients, Eur. J. Heart Fail. 13 (2011) 76–82.
[9] S. Zieman, D. Kass, Advanced glycation end product cross-linking: pathophysiologic role and therapeutic target in cardiovascular disease, Congest. Heart Fail. 10 (2004) 144–149 (quiz 50-1).
[10] R. Candido, J.M. Forbes, M.C. Thomas, V. Thallas, R.G. Dean, W.C. Burns, et al., A breaker of advanced glycation end products attenuates diabetes-induced myocardial structural changes, Circ. Res. 92 (2003) 785–792.
[11] I. Falcao-Pires, N. Goncalves, C. Moura, I. Lamego, C. Eloy, J.M. Lopes, et al., Effects of diabetes mellitus, pressure-overload and their association on myocardial structure and function, Am. J. Hypertens. 22 (2009) 1190–1198.
[12] L. Ernande, C. Bergerot, E.R. Rietzschel, M.L. De Buyzere, H. Thibault, P.G. Pignonblanc, et al., Diastolic dysfunction in patients with type 2 diabetes mellitus: is it really the first marker of diabetic cardiomyopathy? J. Am. Soc. Echocardiogr. 24 (2011) 1268–1275, e1.
[13] C.E. van den Brom, J.W. Bosmans, R. Vlasblom, L.M. Handoko, M.C. Huisman, M. Lubberink, et al., Diabetic cardiomyopathy in Zucker diabetic fatty rats: the forgotten right ventricle, Cardiovasc. Diabetol. 9 (2010) 25.
[14] A.N. Long, S. Dagogo-Jack, Comorbidities of diabetes and hypertension: mechanisms and approach to target organ protection, J. Clin. Hypertens. (Greenwich) 13 (2011) 244–251.
[15] R.M. Lago, P.P. Singh, R.W. Nesto, Diabetes and hypertension, Nat. Clin. Pract. Endocrinol. Metab. 3 (2007) 667.
[16] E. Grossman, F.H. Messerli, Hypertension and diabetes, Adv. Cardiol. 45 (2008) 82–106.
[17] V.P. Singh, A. Bali, N. Singh, A.S. Jaggi, Advanced glycation end products and diabetic complications, Korean J. Physiol. Pharmacol. 18 (2014) 1–14.
[18] B. Yang, D.F. Larson, R. Watson, Age-related left ventricular function in the mouse: analysis based on in vivo pressure–volume relationships, Am. J. Phys. 277 (1999) H1906–H1913.
[19] J. van der Velden, L.J. Klein, M. van der Bijl, M.A. Huybregts, W. Stooker, J. Witkop, et al., Isometric tension development and its calcium sensitivity in skinned myocyte-sized preparations from different regions of the human heart, Cardiovasc. Res. 42 (1999) 706–719.
[20] T.J. Regan, M.M. Lyons, S.S. Ahmed, G.E. Levinson, H.A. Oldewurtel, M.R. Ahmad, et al., Evidence for cardiomyopathy in familial diabetes mellitus, J. Clin. Invest. 60 (1977) 884–899.
[21] I. Russo, N.G. Frangogiannis, Diabetes-associated cardiac fibrosis: cellular effectors, molecular mechanisms and therapeutic opportunities, J. Mol. Cell. Cardiol. 90 (2016) 84–93.
[22] T. Radovits, S. Korkmaz, S. Loganathan, E. Barnucz, T. Bomicke, R. Arif, et al., Comparative investigation of the left ventricular pressure–volume relationship in rat models of type 1 and type 2 diabetes mellitus, Am. J. Physiol. Heart Circ. Physiol. 297 (2009) H125–H133.
[23] T. Radovits, S. Korkmaz, C. Matyas, A. Olah, B.T. Nemeth, S. Pali, et al., An altered pattern of myocardial histopathological and molecular changes underlies the different characteristics of type-1 and type-2 diabetic cardiac dysfunction, J. Diabetes Res. 2015 (2015) 728741.
[24] F.L. Khong, Y. Zhang, A.J. Edgley, W. Qi, K.A. Connelly, O.L. Woodman, et al., 3′,4′-Dihydroxyflavonol antioxidant attenuates diastolic dysfunction and cardiac remodeling in streptozotocin-induced diabetic m(Ren2)27 rats, PLoS One 6 (2011), e22777.

[25] V. Palmieri, B. Capaldo, C. Russo, M. Iaccarino, S. Pezzullo, G. Quintavalle, et al., Uncomplicated type 1 diabetes and preclinical left ventricular myocardial dysfunction: insights from echocardiography and exercise cardiac performance evaluation, Diabetes Res. Clin. Pract. 79 (2008) 262–268.
[26] G.R. Borges, M. de Oliveira, H.C. Salgado, R. Fazan Jr., Myocardial performance in conscious streptozotocin diabetic rats, Cardiovasc. Diabetol. 5 (2006) 26.
[27] S.E. Litwin, T.E. Raya, P.G. Anderson, S. Daugherty, S. Goldman, Abnormal cardiac function in the streptozotocin-diabetic rat. Changes in active and passive properties of the left ventricle, J. Clin. Invest. 86 (1990) 481–488.
[28] M. Laakso, J. Kuusisto, Insulin resistance and hyperglycaemia in cardiovascular disease development, Nat. Rev. Endocrinol. 10 (2014) 293–302.
[29] N. Goncalves, A.F. Silva, P.G. Rodrigues, E Correia, C, Moura, C. Eloy, et al., Early cardiac changes induced by a hypercaloric diet in "subclinical" obesity, Am. J. Physiol. Heart Circ. Physiol (2016), http://dx.doi.org/10.1152/ajpheart.00684.2015.
[30] S.D. Calligaris, M. Lecanda, F. Solis, M. Ezquer, J. Gutierrez, E. Brandan, et al., Mice long-term high-fat diet feeding recapitulates human cardiovascular alterations: an animal model to study the early phases of diabetic cardiomyopathy, PLoS One 8 (2013), e60931.
[31] J.E. Lee, C.O. Yi, B.T. Jeon, H.J. Shin, S.K. Kim, T.S. Jung, et al., Alpha-lipoic acid attenuates cardiac fibrosis in Otsuka Long–Evans Tokushima Fatty rats, Cardiovasc. Diabetol. 11 (2012) 111.
[32] J. Van de Voorde, B. Pauwels, C. Boydens, K. Decaluwe, Adipocytokines in relation to cardiovascular disease, Metab. Clin. Exp. 62 (2013) 1513–1521.
[33] M.R. Movahed, N. Milne, Presence of biventricular dysfunction in patients with type II diabetes mellitus, Congest. Heart Fail. 13 (2007) 78–80.
[34] A. Borbely, J. van der Velden, Z. Papp, J.G. Bronzwaer, I. Edes, G.J. Stienen, et al., Cardiomyocyte stiffness in diastolic heart failure, Circulation 111 (2005) 774–781.
[35] C. Franssen, S. Chen, N. Hamdani, W.J. Paulus, From comorbidities to heart failure with preserved ejection fraction: a story of oxidative stress, Heart (2015).
[36] S.F. Steinberg, Oxidative stress and sarcomeric proteins, Circ. Res. 112 (2013) 393–405.